Supramolecular Chemistry
Publication details, including instructions for authors and subscription information:
http://www.informaworld.com/smpp/title~content=t713649759

Mini review: Fluorescent heteroditopic ligands of metal ions

Lei Zhu[a]; Lu Zhang[a]; Ali H. Younes[a]
[a] Department of Chemistry and Biochemistry, Florida State University, Tallahassee, FL, USA

To cite this Article Zhu, Lei , Zhang, Lu and Younes, Ali H.(2009) 'Mini review: Fluorescent heteroditopic ligands of metal ions', Supramolecular Chemistry, 21: 3, 268 — 283
To link to this Article: DOI: 10.1080/10610270802538298
URL: http://dx.doi.org/10.1080/10610270802538298

Supramolecular Chemistry
Vol. 21, Nos. 3–4, April–June 2009, 268–283

Taylor & Francis
Taylor & Francis Group

Mini review: Fluorescent heteroditopic ligands of metal ions

Lei Zhu*, Lu Zhang and Ali H. Younes

Department of Chemistry and Biochemistry, Florida State University, Tallahassee, FL, USA

(*Received 10 July 2008; final version received 6 October 2008*)

The recent advances in the development of fluorescent heteroditopic ligands of metal ions are reviewed. The scientific endeavour in this area is fuelled partly by the need for sensing technologies that are (1) targeting substances over large concentration ranges and (2) capable of analysing multiple analytes simultaneously. These objectives are largely not attainable using monotopic coordination platforms. The investigations of the fluorescent heteroditopic ligands of metal ions have revealed surprisingly intricate interplays between metal coordination at two different sites and the photophysical states that are accessible through those systems. The chemical complexity of fluorescent heteroditopic ligands of metal ions warrants further investigations on the fundamental science front in order to fully acquire their potential for meeting our practical needs.

Keywords: heteroditopic ligands; fluorescent sensor; fluoroionophore; metal coordination; large concentration range; multiplexed sensing

1. Introduction

The formulation of supramolecular chemistry (*1*) has accelerated the applications of small-molecule-based ditopic ligands for metal ion coordination (*2*, *3*) in the studies of catalysis (*4–12*), molecular recognition (*2*, *13–19*), allosteric chemical systems (*20–34*), molecular self-assemblies (*35–38*) and fundamental aspects of structure and bonding (*39–43*). Not only has the development of ditopic ligands been instrumental as tools in the advancement of many areas in chemistry, but also in challenging us to gain more thorough understanding of the coordination chemistry, photophysical processes and many other fundamental aspects of those delicately designed chemical systems. Selective examples of ditopic ligands of metal ions developed under the above-mentioned contexts are shown in Figures 1–5. Very brief descriptions of each example are included in the figure captions.

In this mini review, a small but rapidly growing class of ditopic ligands, fluorescent heteroditopic ligands, will be described. They are metal coordinating molecules having *two different* binding sites whose multiple (at least three) coordination states are distinguished by their unique fluorescence properties. They are often discussed under the contexts of practical objectives such as sensing or molecular logic functions. In the limited space of this article, attention will be focused primarily upon the fascinating metal coordination-driven photophysical processes embodied in these molecules. Only with a thorough comprehension of the fundamental aspects of these systems can we address the scientific challenges involved in practical objectives in a rational manner.

2. Metal coordination-driven fluorescence modulation

Before the discussion of individual accomplishments in the field of fluorescent heteroditopic ligands, a brief overview of common approaches applied in metal coordination-driven fluorescence modulation (as reflected by the changes of *steady-state fluorescence observables* such as emission wavelength and fluorescence quantum yield) is warranted. Also, a list of leading reviews and books on this topic are cited at the end of this section to satisfy more inquisitive readers. In this section, the metal ions in discussion are assumed to have primarily electrostatic interactions with ligands in both ground and excited states. Ca^{2+} and Zn^{2+} are typical examples. Photophysical processes that involve heavy atom effect and electron or energy transfer between ligand and metal ion are not included.

2.1 Photoinduced electron transfer (PET) and chelation-enhanced fluorescence (CHEF)

A ligand that undergoes intramolecular PET usually has a fluorophore and an electron donor (e-donor) that are covalently linked but electronically insulated in the ground state (*44*). For example, compound **19** has an anthryl group as a fluorophore and a tertiary amino group as the e-donor (Figure 6). Upon excitation, one electron from the tertiary

*Corresponding author. Email: lzhu@chem.fsu.edu

ISSN 1061-0278 print/ISSN 1029-0478 online

DOI: 10.1080/10610270802538298
http://www.informaworld.com

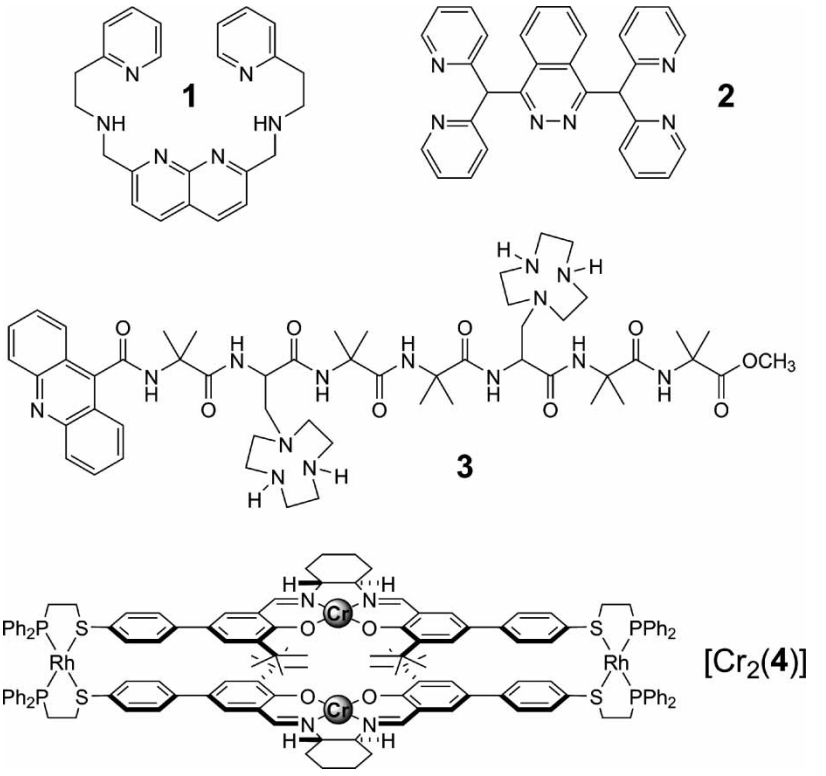

Figure 1. Binuclear catalysis. (**1**): Dizinc complex of **1**, developed by the Lippard group (*9*), is a potent catalyst for tranesterification cleavage of 2-hydroxypropyl-4-nitrophenyl phosphate (HPNP), an RNA model, in buffered aqueous solutions. (**2**): Dinickel complex of **2** is a synthetic model of urease (*8*). (**3**): The dizinc complex of **3** catalyses the hydrolysis of plasmid DNA (pBR322) (*10*). The DNA intercalating acridine moiety conveys additional binding affinity to double-stranded DNA. (**4**): Mirkin's dichromium salen catalyst for epoxide opening by $TMSN_3$ (*12*). The catalytic activity can be enhanced by the addition of CO and Cl^-, which coordinate with Rh to break the Rh—S bonds to allow cooperative catalysis by two Cr(III) centres.

amino group may transfer to the HOMO of the excited anthryl group during its lifetime to form a transient radical cation/anion pair. This transient species undergoes rapid back electron transfer from the LUMO of the reduced anthryl group to the oxidised e-donor so that the ligand returns to the ground state without photon emission. The thermodynamic prerequisite for this type of PET (*45*) is that the HOMO level of the e-donor has to be higher than that of the fluorophore. Upon metal ion coordination, the HOMO level of the e-donating tertiary amino group is lowered to the extent that PET is no longer feasible. Consequently, the non-radiative PET pathway is eliminated, which leads to an enhancement of fluorescence quantum yield (Φ_F). This process is termed CHEF (*46*, *47*).

In addition to fluorescence enhancement upon metal coordination, the common experimental features of a ligand capable of intramolecular PET and CHEF include the following: (1) the coordination of metal ion at the e-donor site has only minor effects on the absorption spectrum of the fluorophore, (2) protonation usually has the same effect as metal coordination to restore the fluorescence of the ligand, (3) a model compound with

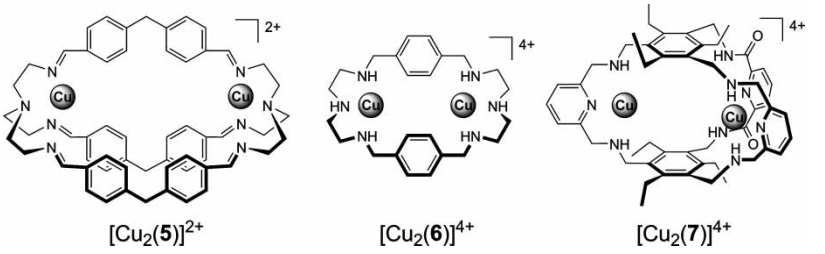

Figure 2. Molecular recognition. (**5**): Lehn's dinuclear cryptate (*2*). The dicopper(I) complex of **5** and its reduced polyamine–Cu(I) complex are receptors for succinate (*14*). (**6**): Dicopper(II) complex of **6** is a receptor for imidazolate (*17*). (**7**): Dicopper(II) complex of **7** is a receptor for the enolate of cyclopentanone (*19*).

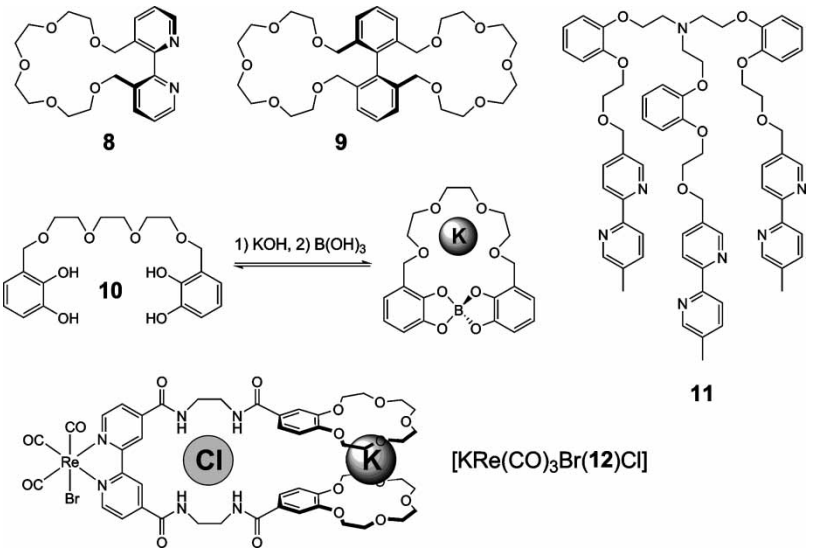

Figure 3. Allosteric chemical systems. (**8**): The coordination of tungsten at 2,2′-bipy site of the allosteric heterodinuclear ligand **8** by Rebek et al. changes the Li^+/K^+ selectivity of the 15C5 (*21*). (**9**): A ditopic ligand that displays positive cooperativity in stepwise coordination of Hg^{2+} (Hill coefficient $n = 1.5$) (*22*, *24*). (**10**): The formation of catecholate–boron complex (boron is a metal analogue here) enables selective binding to K^+(*27*). (**11**): The coordination of Fe(II) with three bipy groups affords a pseudo-cryptand selective for Cs^+(*31*). (**12**): The coordination of Re(I) at the bipy site locks the ligand conformation for simultaneous binding of K^+ and Cl^- (*29*).

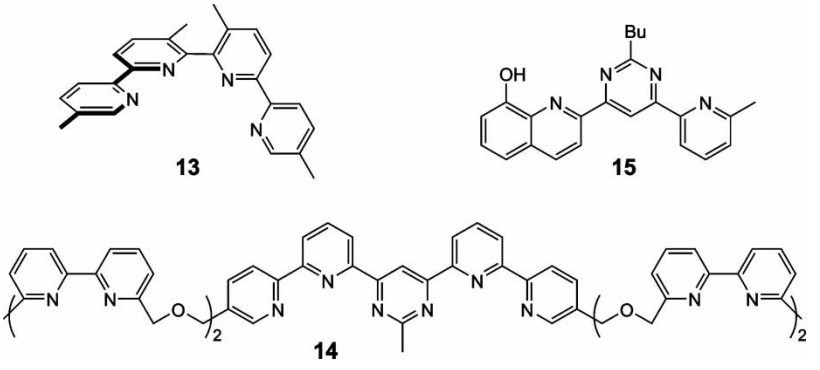

Figure 4. Ligands for self-assembly of helicates or grids. (**13**): 2:2 copper(I) complex affords a helicate precursor (*35*). (**14**): Double-helical or grid-type structures can be accessed by mixing **14** with metal ion combinations of distinct coordination geometry (*37*). (**15**): Zn(II)–Cu(I) heteroditopic complex affords a grid-type structure (*38*).

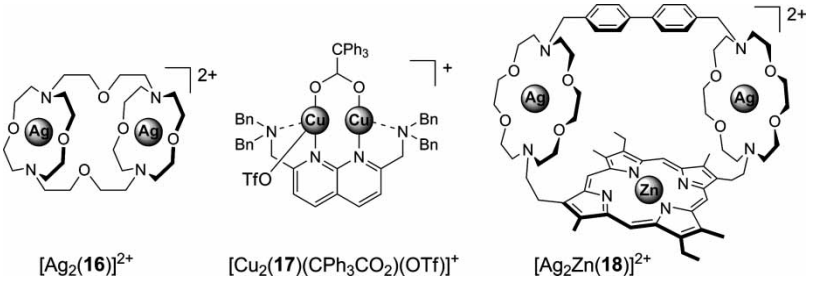

Figure 5. Cation–cation interactions. (**16**): Disilver complex of **16** has Ag–Ag distance 3.876 Å (*39*, *40*). (**17**): A mixed valence dicopper(I, II) complex. Cu–Cu distance is 2.4493 Å (*43*). (**18**): In the trimetallic complex of **18**, PET from the zinc porphrin moiety to the bound silver ions creates a charge-separated state (*41*, *42*).

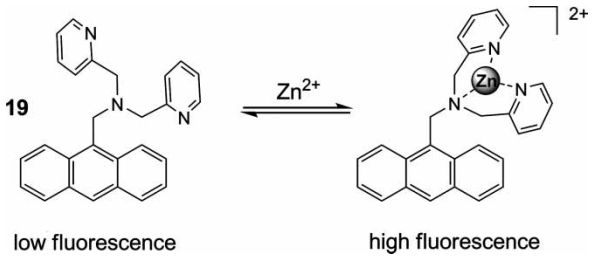

Figure 6. PET and CHEF. In the absence of Zn^{2+} **19** has low fluorescence quantum yield (Φ_F) due to non-radiative PET from the tertiary amino group to the excited anthryl fluorophore. Upon Zn^{2+} coordination, PET is no longer thermodynamically favoured. Consequently, the Zn^{2+} complex has higher Φ_F (*121*).

the e-donor moiety removed should have high Φ_F and (4) cyclic voltammogram of the ligand is expected to have two major oxidation (anodic) peaks for the e-donor and the fluorophore, respectively. The oxidation potential of the e-donor should be lower than that of the fluorophore.

2.2 *Internal or intramolecular charge transfer (ICT)*

An ICT-type fluorophore often undergoes charge redistribution upon excitation. As a result, the dipole moment of the excited state differs from that of the ground state, or the HOMO and LUMO are physically separated in different parts of the fluorophore. If a metal coordination site is incorporated in an ICT fluorophore, in particular if the coordination site is at the positive or negative end of the dipole moment of the excited state, metal binding will profoundly alter the energy gap between ground and excited states, which is reflected as spectral shifts of either absorption or emission, or both.

For example, 7-aminocoumarin undergoes charge redistribution upon excitation. Its ground and excited state structures can be roughly represented using the resonance structures shown in Figure 7(B), which reveals two important pieces of information: (1) the dipole

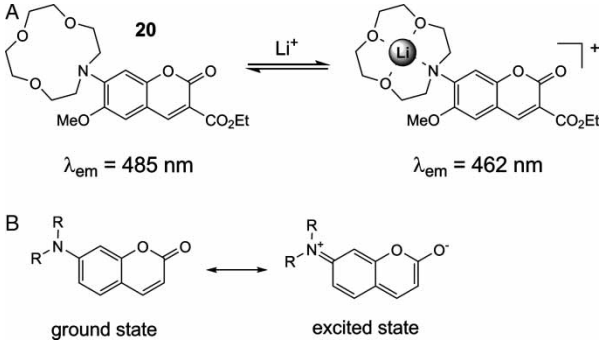

Figure 7. Metal coordination-modulated ICT. (A) An ICT-type ligand **20** undergoes emission hypsochromic shift upon coordinating Li^+ at the positive end of the excited fluorophore (*122*). (B) Two resonance structures of 7-aminocoumarin, which are representative of its ground and excited state structures.

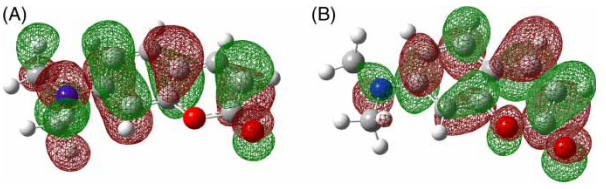

Figure 8. (A) HOMO and (B) LUMO of 7-*N*,*N*-dimethylaminocoumarin, calculated using the B3LYP functional and 6-31G$^+$ (d,p) basis set implemented in the Gaussian 3.0 program (reference in the Supporting Information).

moment of the excited state is larger than that of the ground state and (2) the positive and negative ends of the excited state dipole reside at the nitrogen atom and carbonyl oxygen, respectively. When metal coordination takes place at either the positive or negative ends of the excited state dipole, the excited state is destabilised or stabilised, respectively. Spectroscopically, respective hypsochromic (Figure 7(A)) or bathochromic shifts of emission are expected.

In addition to undergoing spectral shift upon coordinating a metal ion, an ICT-type ligand usually displays absorption or emission solvatochromism (*48*) depending on the ability of solvent dipole to stabilise the ground state relative to the excited state. Frontier molecular orbital computation has been used extensively to visualise the charge redistribution of an ICT fluorophore upon excitation. As shown in Figure 8, relative to the highest occupied molecular orbital (HOMO, Figure 8(A)) of 7-*N*,*N*-dimethylaminocoumarin, the lowest unoccupied molecular orbital (LUMO, Figure 8(B)) is shifted from the amino to lactone side. This figure suggests that during the excitation to elevate one electron from HOMO to LUMO, the electron density of 7-*N*,*N*-dimethylaminocoumarin would shift accordingly to arrive at a charge-transferred state, which agrees with the qualitative conclusion drawn from analysing the resonance structures in Figure 7(B).

2.3 *Excited state intramolecular proton transfer (ESIPT)*

In an ESIPT system, during the lifetime of the excited state of the ligand (e.g. **21**-enamine, Figure 9), it undergoes an ultrafast (e.g. as short as 50 fs (*49*)) tautomerisation to afford a phototautomer (e.g. **21**-imino). which then decays radiatively (*50*). Large Stokes shifts (*51*) and negative fluorescence solvatochromism (*52*, *53*) are often observed in ESIPT systems. When metal coordination occurs, the accompanying deprotonation eliminates ESIPT. Consequently, the emission from the metal complex resembles the fluorescence from the deprotonated ligand, which differs from that of the phototautomer. Caution needs to be applied when interpreting a possible ESIPT system in an aqueous solution because hydrogen bonding of the ligand

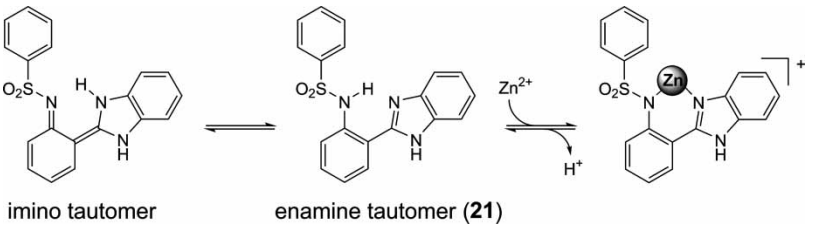

Figure 9. Excited state intramolecular proton transfer (ESIPT). 2-(2′-Tosylaminophenyl)benzimidazole **21** (middle) undergoes ESIPT in an aqueous solution in the absence of metal ion to result in fluorescence from the imino phototautomer (left). Upon Zn^{2+} coordination, ESIPT is disrupted, which restores fluorescence from the native deprotonated **21** (right) (*50*, *123*).

with solvent molecules may severely disrupt the ESIPT process (*54*).

2.4 Excimer/exciplex formation

Fluorophores may form excited/ground-state transient complex upon excitation. Such a complex is termed an excimer (between identical molecules) or an exciplex (between different molecules). Pyrene (Figure 10) is known to form an excimer that emits at ~475 nm as a structureless band. The excitation spectrum of pyrene excimer still resembles the structured absorption spectrum of pyrene. Due to its bimolecular nature, the formation of excimer is concentration dependent. Metal coordination may be utilised to bring two pyrene moieties into close proximity so that the effective molarity of pyrene groups is high enough to give rise to a strong excimer emission.

In addition to the four photophysical processes discussed above, other approaches that have been applied in devising fluorescent reporters for metal ions include metal coordination-effected increase in the energies of singlet or triplet $n-\pi^*$ states relative to the fluorescent $\pi-\pi^*$ singlet excited state (*55–57*), conformational rigidification of fluoroionophores (*58–60*) and modulation of fluorescence resonance energy transfer (FRET) (*61*). Interested readers are directed to the cited references and leading reviews (*44*, *62–68*) in this area.

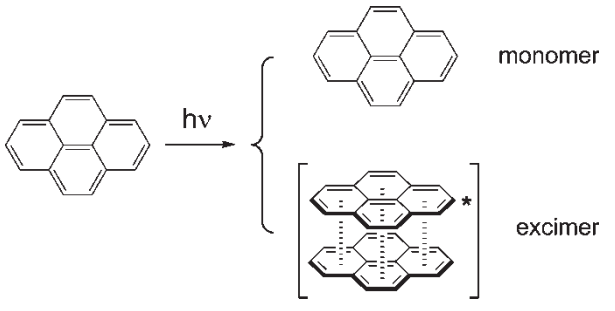

Figure 10. Pyrene excimer formation.

3. Fluorescent heteroditopic ligands of metal ions

The real-world motivation behind the development of fluorescent heteroditopic ligands of metal ions is to achieve quantitative metal ion analysis over large concentration ranges and the simultaneous detection and quantification of two different metal ion analytes. These goals are largely unattainable via monotopic or homoditopic (*69–74*) systems. Depending on the identities and/or quantities of the metal ions present, a fluorescent ditopic ligand is capable of offering at least three coordination states (see sections below) that are associated with three different photophysical processes upon excitation. For all practical purposes, the scientific objectives are (1) achieving the largest contrast possible in terms of fluorescence observables such as emission wavelength and intensity between the three coordination states and (2) spacing the binding affinities and selectivities of the two coordination sites judiciously, so that under one given condition only two or one species dominate in solution. Attaining these two goals mandate thorough understanding of the coordination chemistry and the metal coordination-driven photophysical processes involved in these chemical systems. In this section, the steady-state photophysics and coordination chemistry of a few examples will be described with the realisation that development of fluorescent heteroditopic ligands is still a young area and the stated objectives have yet to be accomplished.

3.1 Group 1: Ligands capable of forming two different mononuclear complexes

As illustrated in Figure 11, fluorescent heteroditopic ligands in the first group are capable of forming two different mononuclear complexes to result in three coordination states. They undergo distinct relaxation processes upon excitation, which may or may not afford different fluorescence observables.

Compound **22**, prepared by Kim et al. (*75*) (Figure 12), was built on a 1,3-alternate calix[4]arene scaffold (*76*, *77*). A pseudo-15-crown-5 (15C5) and a pseudo-monoaza-15C5 constitute the top and bottom parts, respectively,

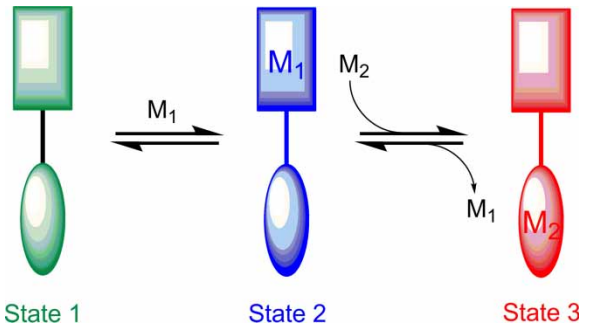

Figure 11. A fluorescent heteroditopic ligand having three coordination states: free ligand (L) and two mononuclear complexes M_1L and M_2L.

of the ligand. An appended pyrene group was used to report metal binding event through fluorescence modulation. The tertiary amino group was postulated to undergo PET to the excited pyrene so that the free ligand is only weakly fluorescent. It should be noted that the alkoxybenzene components in the calix[4]arene structure may also serve as PET donors. When Ag^+ was introduced, it presumably selectively coordinated to the softer monoaza-15C5 cavity, which raised the oxidation potential of the tertiary amino group to stop PET and revive the fluorescence (CHEF). When the Ag^+ complex of **22** was exposed to K^+, K^+ presumably entered the top 15C5 site. The dinuclear complex $[AgK(\mathbf{22})]^{2+}$ was disfavoured due to the electrostatic repulsive interactions between K^+ and Ag^+. Therefore, Ag^+ exited the ligand to afford the mononuclear K^+ complex of **22**. The PET channel was reopened to result in fluorescence reduction. The formation of the 1:1 Ag^+ complex was confirmed using Job's method of continuous variation and high-resolution FAB-MS. However, the proposed binding sites of Ag^+ and K^+ ions in the complexes may require more data (in addition to fluorescence, e.g. NMR studies) to confirm. Another observation worth noting in this study is that the formation of the Cu^{2+} complex is accompanied by pronounced fluorescence enhancement, which is contrary to most other observations that Cu^{2+} coordination causes fluorescence quenching (*47*, *78*).

In an extension from their previous contribution, Kim et al. studied **23** (*79*) where the fluorescence reporting group, 9-cyanoanthracene, was appended to the pseudo-18C6 (top) side instead (Figure 13). The *o*-dialkoxybenzene moiety, which is part of the pseudo-18C6, served as the PET quencher (*70*, *71*, *80*, *81*). The oxidation potential of the *o*-dialkoxybenzene was raised upon Cs^+ coordination at the 18C6 site to result in an enhancement of fluorescence (CHEF effect). As Cu^{2+} bound at the smaller, softer monoaza-15C5 site, Cs^+ was expelled. The reopened PET channel as well as the known quenching ability of the paramagnetic Cu^{2+}(*78*) may have collectively contributed to the observed fluorescence quenching of the monocopper(II) complex of **23**.

Recently, Kim's group developed **24,** which used coordination-driven modulation of pyrene excimer emission to signal the presence of Pb^{2+}, a metal ion of environmental importance (*82*) (Figure 14). While **24** was in its free form, a strong emission band from the pyrene excimer along with moderate emission from the monomer was observed when excited at 344 nm in acetonitrile. In the presence of Pb^{2+}, both the excimer and monomer emission was quenched. It was postulated that Pb^{2+} coordinated with the two amide carbonyl groups of **24**, which hindered the excimer formation upon excitation. The selective binding of Pb^{2+} with the carbonyl oxygen atoms was supported by binding studies using ^1H NMR. Furthermore, the monomer emission may have been quenched through electron transfer from excited pyrene to the Pb^{2+}-coordinated amide bonds, and/or due to heavy

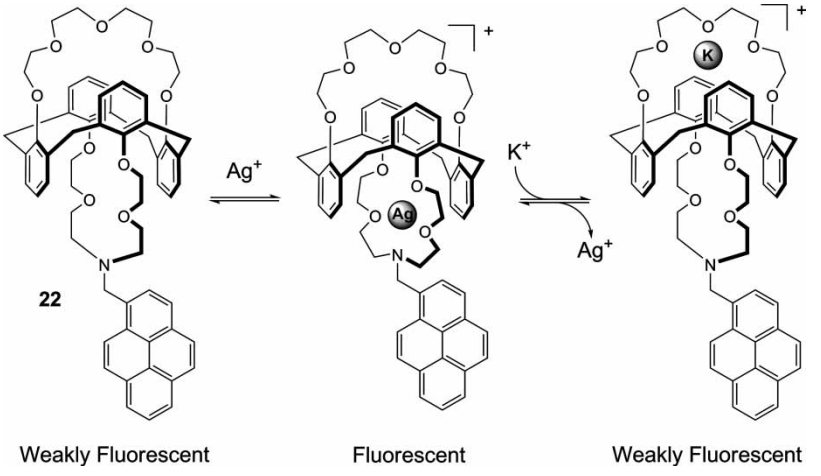

Figure 12. Fluorescence of **22** (observed at 389 nm in ethanol) is enhanced upon coordination with Ag^+. The introduction of K^+ displaces Ag^+ to afford the mononuclear K^+ complex that fluoresces weakly, similar to that of free ligand **22** (*75*).

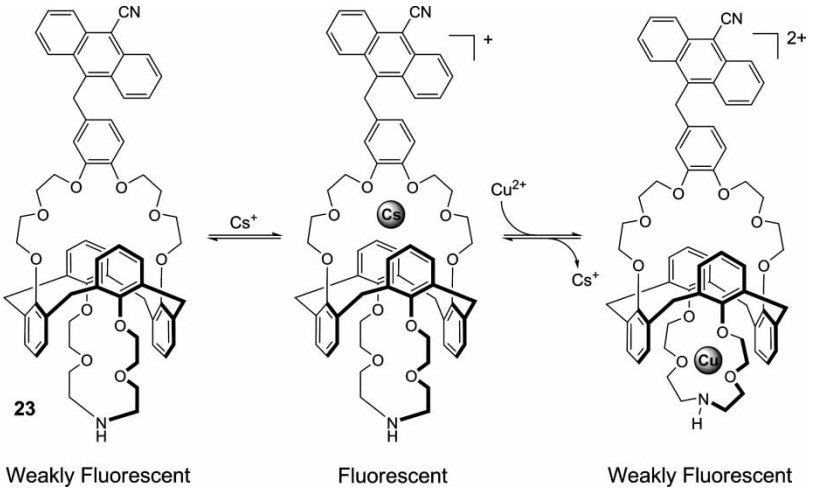

Figure 13. Fluorescence of **23** (observed at 450 nm in ethanol–dichloromethane, 9:1 v/v) is enhanced upon coordination with Cs^+. The introduction of Cu^{2+} displaces Cs^+ to afford the mononuclear Cu^{2+} complex that fluoresces weakly (*79*).

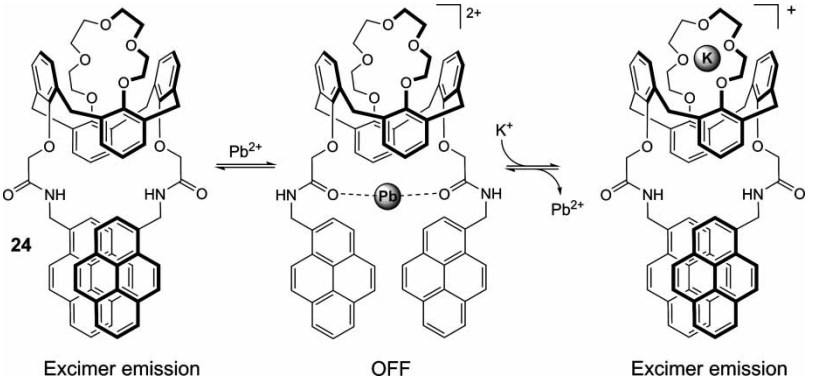

Figure 14. Ligand **24** displays emission from pyrene excimer (observed at 470 nm in acetonitrile), which is quenched upon formation of the Pb^{2+} complex. The binding of K^+ in the top crown expels Pb^{2+}, which restores the pyrene excimer emission (*82*).

atom effect exerted by Pb^{2+}. When K^+ was introduced into the system and bound to the 18C6 cap, Pb^{2+} was expelled to restore the excimer formation. The selectivity of **24** to K^+ was demonstrated using an acyclic control compound lacking the crown cap. The fluorescence from pyrene excimer of the control compound quenched upon addition of Pb^{2+}, however, was not restored upon introduction of 10,000-fold excess of K^+.

3.2 Group 2: Ligands capable of forming both mono- and dinuclear complexes

The three examples from the Kim group where the free form and two different mononuclear complexes constitute the three coordination states of a heteroditopic ligand have begun to reveal the complexity of the coordination chemistry and associated photophysical processes of heteroditopic systems. The potential of the ligands in group 1 for technological development, i.e. to associate their chemical behaviours to the solutions of practical problems, has not been systematically evaluated (although **24** was developed as an on–off switchable sensor of Pb^{2+} and K^+). Different from the compounds in group 1, the ligands in the second group are capable of forming dinuclear complexes (Figure 15). Free ligand, mono- and dinuclear complexes are associated with three different

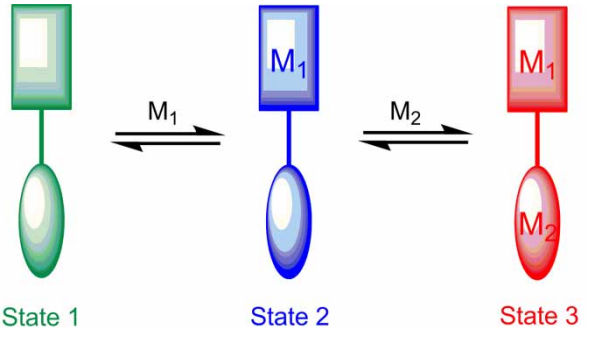

Figure 15. Three coordination states of a fluorescent heteroditopic ligand: free ligand (L), mononuclear complex M_1L and dinuclear complex M_1M_2L.

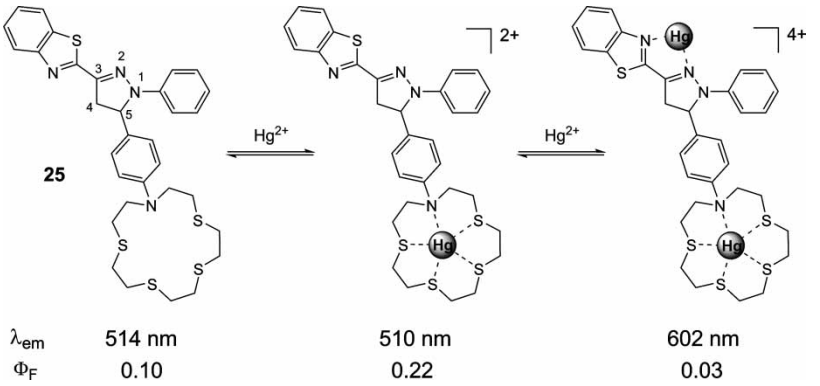

Figure 16. Three different coordination states of **25** at various Hg^{2+} concentrations in acetonitrile (*83*). The numbering scheme for pyrazoline is shown. The emission band maxima (λ_{em}) and fluorescence quantum yields (Φ_F) of three species in acetonitrile are listed.

fluorescence states. This ditopic platform offers opportunities for the development of sensing technologies that are effective over large concentration ranges or capable of simultaneous analysis of two metal ion analytes.

Compound **25** was investigated by Rurack et al. on its cation complexation-mediated photophysical properties (*83*) (Figure 16). The *N*-phenyl-tetrathia-monoaza-15-crown-5 ($AT_4$15C5) was designed as e-donor to undergo PET to the excited benzothiazolyl-pyrazoline fluorophore (*84–88*). Upon addition of $Hg(ClO_4)_2$ in acetonitrile, a CHEF effect was observed as the Φ_F of **25** increased from 0.10 to 0.22. However, with the introduction of excess Hg^{2+}, both absorption and emission spectra of **25** underwent a pronounced bathochromic shift characteristic of metal coordination at the negative end of the dipole of an excited ICT type fluorophore. It was interpreted that excess Hg^{2+} coordinated at the bidentate site within the benzothiazolyl-pyrazoline fluorophore [both nitrogen and sulphur atoms of benzothiazolyl may coordinate Hg^{2+}; however, coordination between Hg^{2+} and sulphur in a thienyl group has not been shown to be selective (*89*, *90*)].

This observation by Rurack et al. is one of the first examples where sequential coordination of a heteroditopic ligand led to three distinct fluorescence responses (*91*). At the end of that article, the investigators suggested that such a strategy could be used to develop sensing technologies effective over large concentration ranges and molecular logic functions. This prospect has motivated many researchers to study various heteroditopic systems that may achieve fluorescence contrasts (in terms of fluorescence quantum yield and emission wavelength) of the three coordination states that are appropriate for individual applications.

Compound **26**, also investigated by Rurack et al. (*92*), is a combination of two fluorophores with distinct excited state behaviours (Figure 17). The amino-substituted benzothiazole (top half) has a highly emissive, charge-transferred planar excited state (ICT); the amino-stilbenoid structure (bottom half) is known to be moderately emissive from a twisted intramolecular charge-transferred excited state (TICT) (*93*). Also, the electron-rich amino-stilbenoid half weakens the e-acceptor character of the benzothiazole group, which reduces the fluorescence quantum yield (Φ_F) of **26**. At the same time, two distinct macrocyclic coordination motifs are included. The monoaza-15-crown-5 (A15C5) has high affinities to hard metal ions such as Ca^{2+} (*94*); its tetrathia version ($AT_4$15C5) prefers soft ions such as Ag^+.

Upon exposure to Ag^+, the soft $AT_4$15C5 site is coordinated. The cationic nature of the bottom half of **26** enhances the electron-accepting capacity in respect of the aminobenzothiazole fluorophore. Consequently, the fluorescence of **26** is enhanced. As Ca^{2+} ion is introduced to the solution of the Ag^+ complex, the A15C5 site is occupied by Ca^{2+}. The coordination of Ca^{2+} with the e-donor amino group depopulates the ICT state, which results in greatly reduced fluorescence. This system may serve as a foundation for constructing sensors for detecting and quantifying two different metal ions in the same sample.

2-(2′-Hydroxyphenyl)benzoxazole (HBO) motif is known to undergo ESIPT, which may be terminated through metal coordination. **27** was prepared by Arai et al., which undergoes two-step coordination with Zn^{2+} in a buffered aqueous solution (40 mM HEPES, 100 mM KCl (pH 7.2)) (*95*) (Figure 18). The absorption spectrum of **27** underwent a blue shift followed by a red shift during the course of a Zn^{2+} titration, which suggests that coordination at the electron-donating aminophenol triacetate (APT) site occurs prior to binding at the electron-accepting HBO site. The fluorescence intensity of **27** ($\lambda_{max} = 430$ nm) dropped slightly over a bathochromic shift to ~450 nm as the first-step Zn^{2+} coordination at APT site occurred. The fluorescence intensity reduction was partly due to the decrease in absorbance at the excitation wavelength (360 nm). As the dizinc complex of **27** formed at higher Zn^{2+} concentrations, a dramatic fluorescence enhancement at 451 nm was observed. This enhancement was attributed initially to the termination of ESIPT as the HBO site was coordinated. However, a later

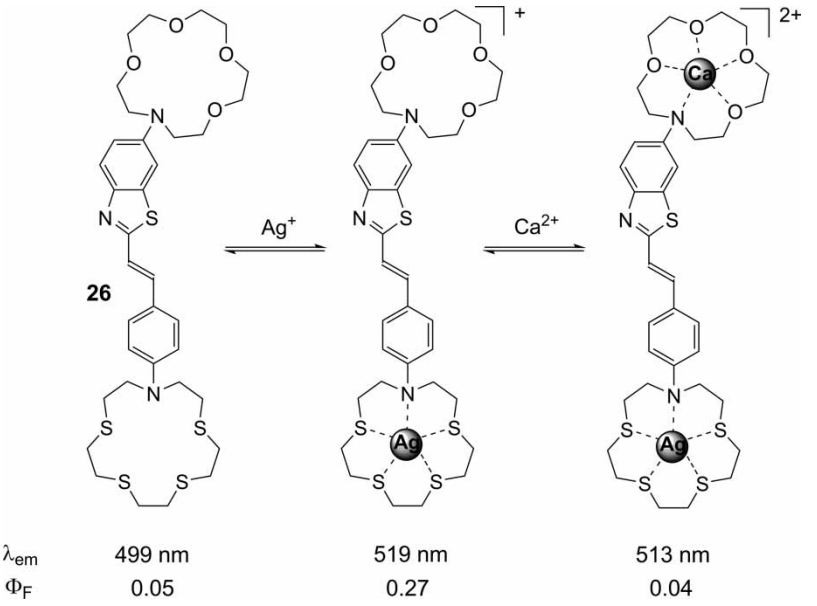

Figure 17. Ligand **26** undergoes sequential coordination with Ag^{+} and Ca^{2+}. The emission band maxima (λ_{em}) and fluorescence quantum yields (Φ_F) of three species in acetonitrile are listed.

investigation using laser photolysis failed to show the keto tautomer of **27** (*96*) under the buffered aqueous conditions. The bathochromic shift that **27** underwent upon HBO coordination may have been caused by coordination-promoted deprotonation of the phenyl hydroxyl group (*97*). Zn^{2+} coordination at the HBO site restricted the rotation of the C—C bond, which may have slowed down the rates of non-radiative processes to contribute to the observed fluorescence quantum yield enhancement (*58*, *59*).

Compound **28** was investigated by the Resch-Genger group (Figure 19) (*98*). Recognising the need for fluorescent ditopic ligands for metal ion detection over large concentration ranges and technologies for simultaneous detection of multiple analytes, **28** was studied as a model system for evaluating the design principle of such ligands based on ICT type fluorophores. Compound **28** contains two metal binding sites: monoaza-15-crown-5 (A15C5) and 2,2′:6′,2″-terpyridine (tpy). The aromatic scaffold is a typical ICT type fluorophore where the 4-aminophenyl is the e-donor and the tpy group is the e-acceptor. A15C5 binds with hard metal ions (groups I and II) tightly, whereas tpy is expected to be selective for transition metal ions of intermediate hardness. However, when Ca^{2+} was titrated into a solution of **28**, a bathochromic shift of absorption spectrum (350–394 nm) took place, which suggested that Ca^{2+} preferentially bound at the e-acceptor site tpy. As Ca^{2+} became more concentrated, the absorption band centred at 394 nm disappeared, signalling the coordinating of Ca^{2+} at the A15C5, e-donor site. The fluorescence quantum yield of **28** in acetonitrile decreased along with a bathochromic shift as the tpy site was being occupied. When the Ca^{2+} concentration was high and, presumably, the A15C5 site was coordinated, the fluorescence underwent a slight hypsochromic shift and approximately three-fold enhancement.

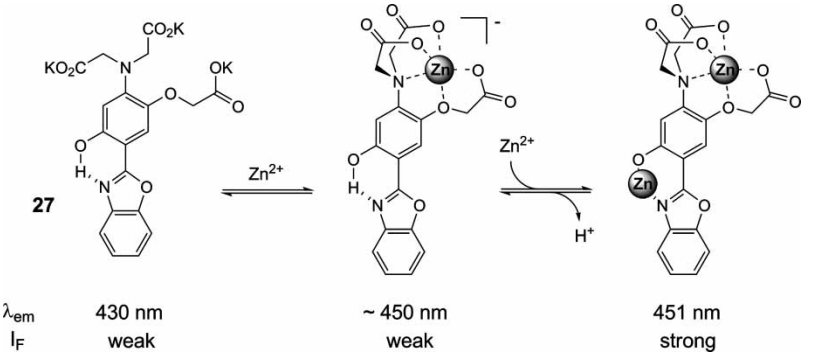

Figure 18. Compound **27** forms monozinc and dizinc complexes as Zn^{2+} concentration increases (*95*). The emission maxima (λ_{em}) in an aqueous solution (40 mM HEPES, 100 mM KCl (pH 7.20)) are listed. I_F, fluorescence intensity.

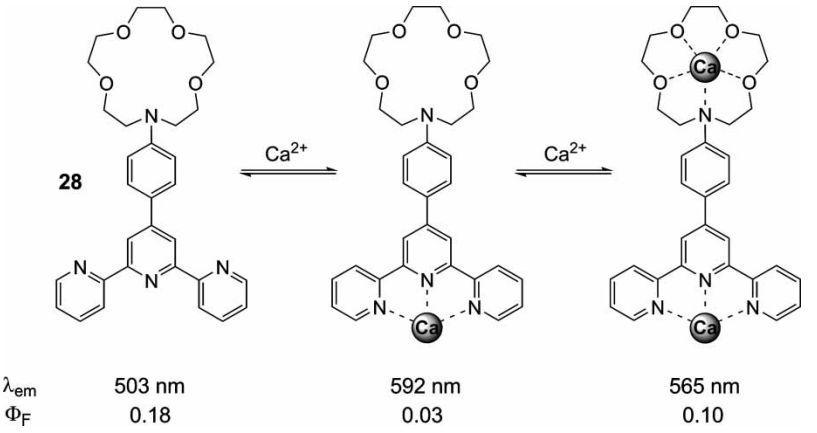

Figure 19. Compound **28** forms mono- and dicalcium complexes as Ca^{2+} concentration increases. The emission maxima (λ_{em}) and fluorescence quantum yields (Φ_F) of the three species in acetontrile are listed.

Bunz's cruciform **29** showed beautiful optical modulation when interacting with Zn^{2+} at different concentrations in dichloromethane (Figure 20) (*99*). Frontier molecular orbital calculations showed that the HOMO and the LUMO are disjoint (or physically separated, Figure 21) (*100*). Therefore, the excitation of **29** mandates a charge-separated excited state. In the presence of Zn^{2+}, the coordination sites on the HOMO-residing bis(aminostyryl)benzene branch

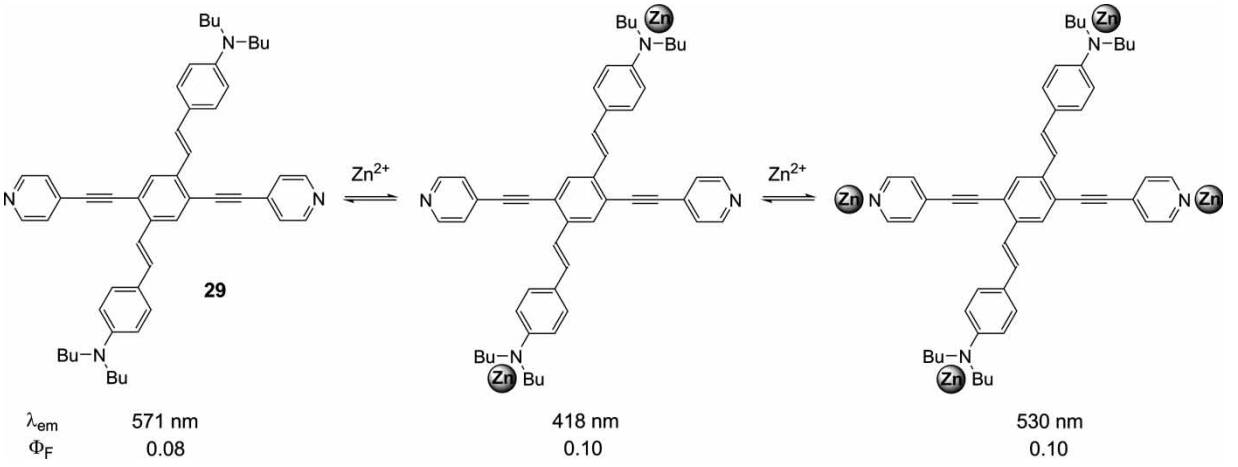

Figure 20. Compound **29** forms dizinc and tetrazinc complexes as Zn^{2+} concentration increases (*99*). The emission maxima (λ_{em}) and fluorescence quantum yields (Φ_F) of the three species in dichloromethane are listed.

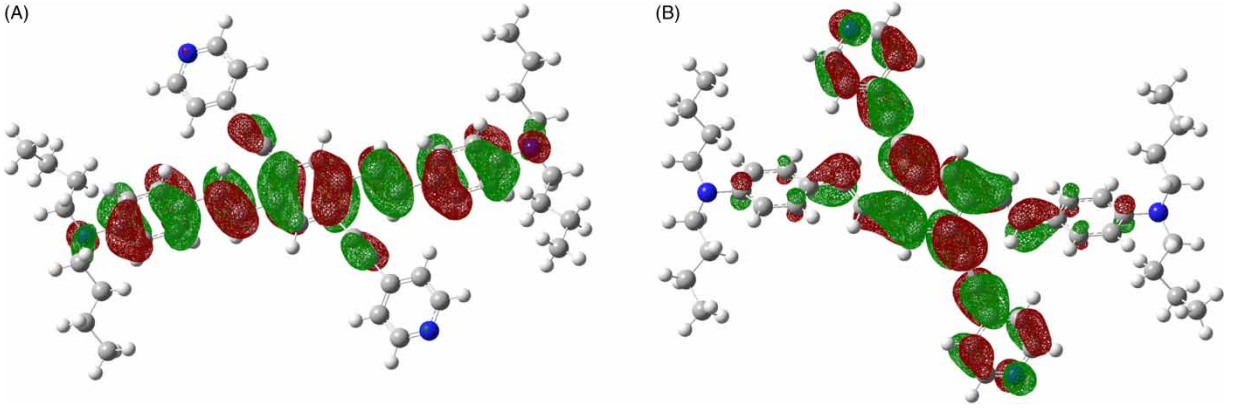

Figure 21. (A) HOMO and (B) LUMO of **29**, calculated using the HF functional and 6-31G (d) basis set implemented in the Gaussian 3.0 program (reference in the Supporting Information).

were occupied first. The selective binding was confirmed by a ^{1}H NMR titration study (*100*). The increased HOMO–LUMO energy gap due to the stabilisation of HOMO upon coordination resulted in a large hypsochromic (blue) shift of the fluorescence emission. With increasing concentration of Zn^{2+}, the LUMO-residing bis(pyridylethynyl)benzene branch of **29** was also coordinated, thus decreasing the HOMO–LUMO gap to shift the spectrum back to longer wavelength.

The pincer ligand **30** developed by the Koskinen group utilises the preferential coordination of salen ligand to transition metals such as Zn^{2+} to create a second, crown-ether-type pseudo-macrocycle for further coordination with alkali metals (Figure 22) (*101*). The coordination behaviour was reminiscent of designs shown in compounds **10**–**12** (Figure 3). In this case, however, the coordination event can be reported by fluorescence modulation of the two appended pyrene groups. The Zn^{2+} coordination resulted in greatly enhanced emission centred at 475 nm, which is characteristic of the emission from the pyrene excimer. The further coordination of [Zn(**30**)] with Li^+ decreased the fluorescence intensity. No spectral shift was observed. The mechanism of Li^+-dependent fluorescence modulation is unclear. Li^+ coordination may have reduced the affinity between salen and Zn^{2+} due to electrostatic interactions, and/or subtly changed the conformation of the pincer structure to disrupt the excimer formation.

Fukuzumi et al. at Osaka University found that the coordination of 2,3,5,6-tetrakis(2-pyridyl)pyrazine (TPPZ, **31**) with transition metal ions such as Sc^{3+} and Zn^{2+} led to fluorescence changes (Figure 23) (*102*, *103*). The free ligand is not fluorescent because the triplet n,π* state

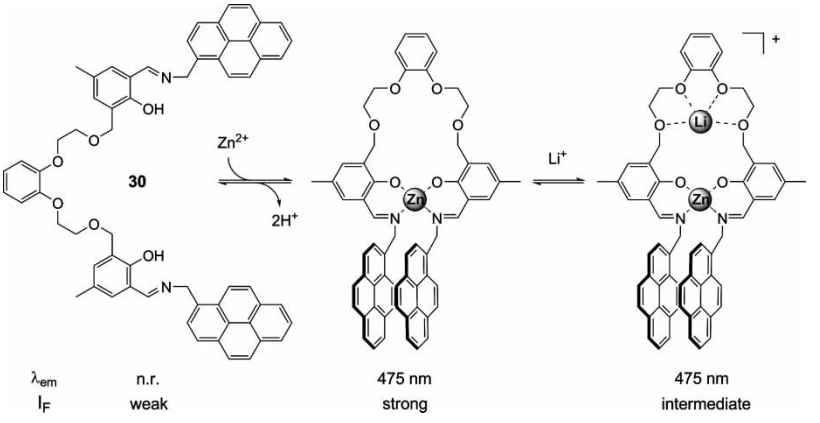

Figure 22. The salen moiety of **30** coordinates with Zn^{2+} in MeOH/THF (1:1) to form a pseudo-crown, which selectively binds with Li^+(*101*).

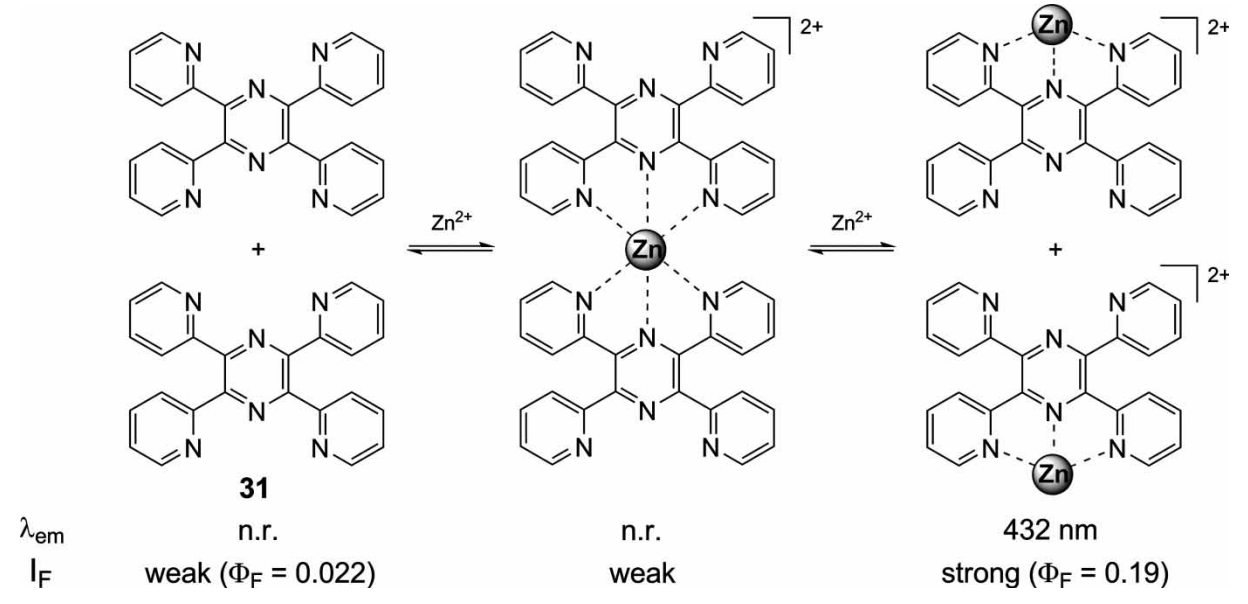

Figure 23. Compound **31** forms a weakly emissive 2:1 (ligand:metal) complex with Zn^{2+} in acetonitrile, which is broken up to afford a highly emissive 1:1 complex when Zn^{2+} concentration is high (*102*, *103*). n.r., not reported.

is efficiently populated upon excitation. In the presence of Zn^{2+} at low concentration, the formation of 2:1 (ligand:Zn^{2+}) complex did not lead to fluorescence enhancement, presumably due to the inability of the 2:1 complex formation to depopulate $^3(n,\pi^*)$ by raising its energy higher than the $^1(\pi,\pi^*)$ state. As Zn^{2+} concentration was increased to afford the mononuclear complex, however, the Lewis acidity of Zn^{2+} in the mononuclear complex was postulated high enough to render the $^1(\pi,\pi^*)$ state as the lowest excited state. Consequently, the 1:1 complex of **31** became highly emissive. Both 2:1 and 1:1 complexes of **31** were characterised by ESI–MS.

The strategy utilised by Fukuzumi differs from the main theme of this review. Instead of using a ditopic ligand, a pseudo-monotopic ligand (TPPZ) capable of forming both 2:1 (ligand:metal) and 1:1 complexes was explored to create three photophysically distinct coordination states (*104*). However, the fluorescence states of the free ligand and 2:1 complex are similar (both display weak fluorescence). Further effort is warranted in designing monotopic ligands that give rise to fluorescently distinct multiple coordination states.

Qian et al. constructed a heteroditopic ligand (**32**) for cadmium(II) by appending two piperazine moieties at the 2 and 7 positions of a 1,8-naphthyridine scaffold (Figure 24) (*105*). The installation of a butylamino group at position 4 renders the ligand fluorescent. Upon titrating Cd^{2+} into an ethanol–water (pH 7) solution of **32**, a distinct two-step fluorescence modulation was observed. The initial decrease in fluorescence intensity was followed by a rising band at a longer wavelength (450 nm). A stepwise coordination process was hypothesised, where upon increasing Cd^{2+} concentration, the 1,8-naphthyridine site was preferentially occupied, which presumably stabilised the ICT excited state of the fluorophore. As a result, the overall bathochromic shifts of absorption and fluorescence spectra of **32** were observed over the course of the Cd^{2+} titration. Further increase in Cd^{2+} concentration enabled the formation of the dinuclear complex of **32**, where the two piperizine moieties participated in binding. The enhancement of fluorescence intensity observed at this stage was attributed to the CHEF effect upon metal coordination at the four tertiary nitrogen atoms that may serve as e-donors to quench the fluorescence in the absence of metal ions. The reduction in fluorescence intensity at the early stage of the titration, however, was not specifically addressed.

This study offers an interesting coordination-driven fluorescence modulation process involving a sequential coordination of a heteroditopic ligand [a chromophoric heteroditopic 1,8-naphthyridine derivative was reported as a Hg^{2+} sensor (*106*)]. A plausible explanation on Cd^{2+} coordination-modulated fluorescence change was proposed; however, more investigation is required to substantiate it. The unusual four-membered coordination ring motif proposed for the mono-Cd^{2+} complex has been identified in an X-ray crystal structure of a 1,8-naphthyridine–Ir(III) complex (*107*). However, the acyclic, mono- or dinuclear complexes (see below) of various transition metals (Ru (*108*), Cu, Ni, Zn, Co

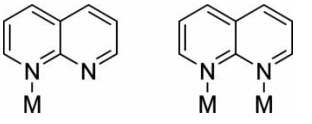

(*9*), Ag (*109*), Fe (*110*), Rh (*111*), etc.) are more commonly observed. Free ligand **32** did not exhibit PET, as suggested by the pH profile of fluorescence. It is likely that (1) the relatively high HOMO (*45*, *88*, *112*, *113*) of 4-butylamino-substituted 1,8-naphthyridine and (2) the dipolar nature of the excited state (*114–116*) reduced the rate of PET. Upon coordinating the first Cd^{2+} to form the proposed mononuclear complex, the HOMO of the fluorophore is lowered to afford a more efficient PET process, which results in fluorescence quenching. The coordination at the tertiary nitrogen atoms at high Cd^{2+} concentrations, on the other hand, lowers the HOMO of the electron donors of the PET, thus reviving the fluorescence (CHEF).

Our group is interested in developing fluorescent probes for Zn^{2+} with both low detection limit and large

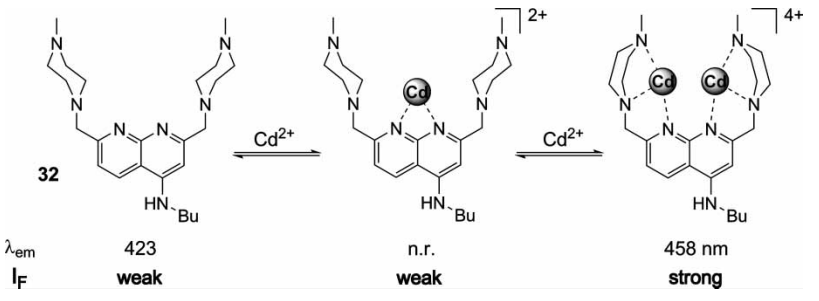

Figure 24. The coordination between **32** and Cd^{2+} induces a consistent bathochromic shift of emission. The fluorescence intensity drops initially before increasing to saturation as the concentration of Cd^{2+} increases, suggesting a stepwise coordination to afford the dinuclear complex (*105*).

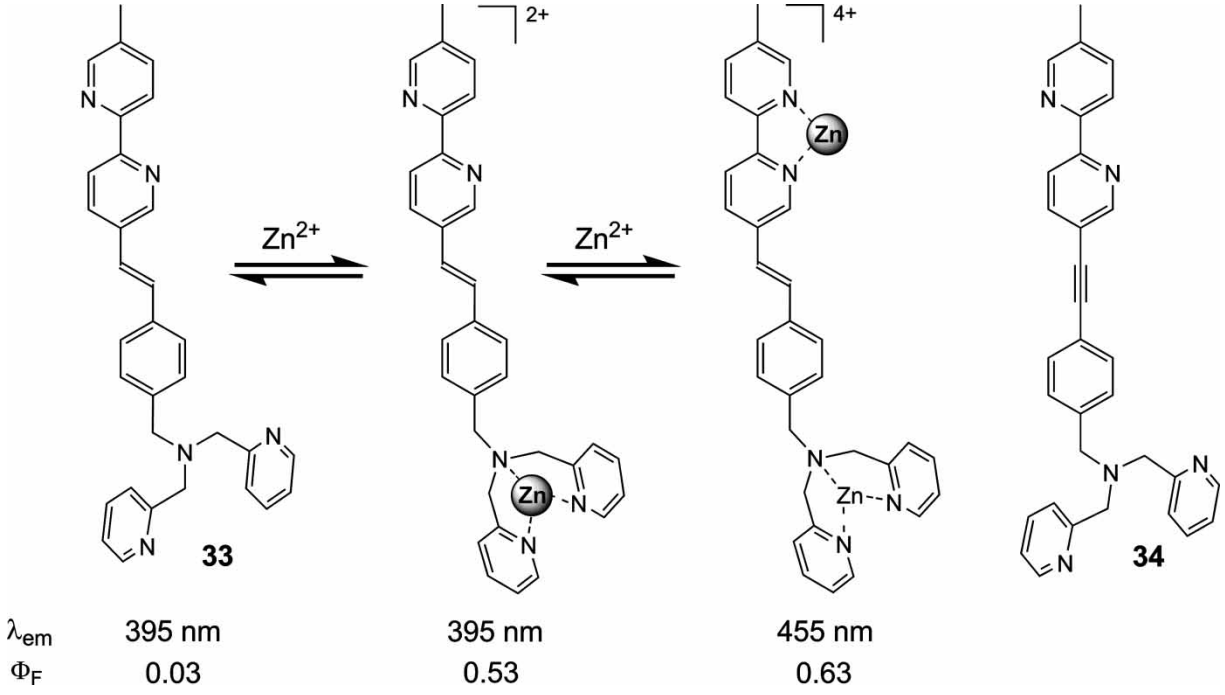

Figure 25. Compound **33** undergoes stepwise coordination with Zn^{2+} in acetonitrile to afford three coordination states with distinct fluorescence properties (*118*).

effective concentration ranges (*97*, *117*, *118*). Compound **33** was reported as a model system for designing probes for Zn^{2+}, which cover large concentration ranges (Figure 25) (*118*, *119*). **33** includes two metal coordination sites: dipicolylamino (DPA) and 2,2′-bipyridyl (bipy) groups. The bipy group is incorporated in a phenylvinyl–bipy fluorophore. In the absence of Zn^{2+}, PET from the tertiary amino group in DPA to the excited stilbenoid fluorophore quenches the fluorescence. As Zn^{2+} concentration increases, Zn^{2+} enters the high-affinity DPA group to result in CHEF. As Zn^{2+} concentration is high enough to coordinate the low-affinity bipy site, the coordination stabilises the charge-transferred excited state to give rise to a bathochromic shift of emission (from 395 to 455 nm). Overall, upon increasing Zn^{2+} concentration in acetonitrile, **33** underwent fluorescence enhancement followed by bathochromic shift of the emission band (Figure 26). Positive fluorescence solvatochromism observed for fluorophores with arylvinyl–bipy or arylalkynyl–bipy structures supports the postulated charge-transferred

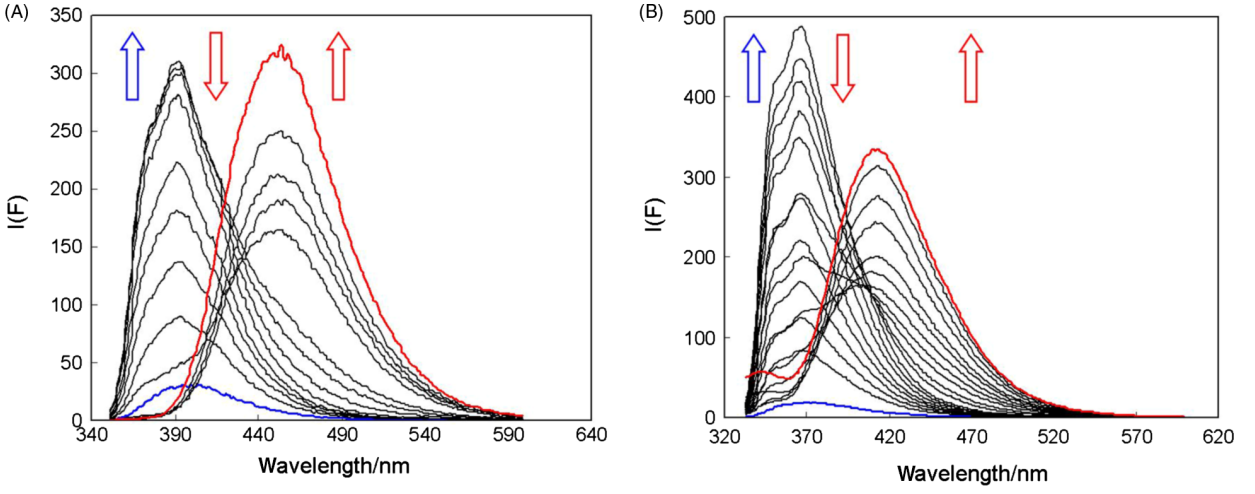

Figure 26. Fluorescence spectra of (A) **33** (2.0 μM, $\lambda_{ex} = 339$ nm) and (B) **34** (2.0 μM, $\lambda_{ex} = 321$ nm) in MeCN (DIPEA: 2.0 μM, TBAP: 5.0 mM) upon addition of $Zn(ClO_4)_2$. The blue arrow presents the initial fluorescence enhancements; the red arrows represent the following bathochromic shifts. The blue and red spectra were taken in the absence of Zn^{2+} and in the presence of (A) 5.6 μM and (B) 8.8 μM of Zn^{2+}, respectively (*118*, *120*).

excited states (*118*). Cyclic voltammetry experiments suggest that PET is highly efficient in **33** and **34** in the absence of Zn^{2+}, which leads to large CHEF effect upon coordinating Zn^{2+} at the DPA sites (*120*).

In order to circumvent the photo-instability of stilbenoid fluorophores featured in **33** so that this class of fluorescent heteroditopic ligands can be applied in quantitative sensing/imaging technologies, the alkynyl analogues such as **34** were investigated (Figure 25) (*120*). Similarly, the photochemically stable **34** undergoes fluorescence enhancement followed by emission bathochromic shift during a course of Zn^{2+} titration (Figure 26(B)). Furthermore, the arylalkynyl–bipy fluorophores have higher oxidation potentials than their vinyl analogues, which led to more efficient PET in the absence of Zn^{2+}. Consequently, the CHEF effect of **34** is greatly amplified over its vinyl analogue **33**.

Our ligand scaffold utilises the combination of metal coordination modulated PET/CHEF and ICT to achieve three distinct fluorescence states. The first-step coordination to afford the mononuclear complex is a fluorogenic event resulted from CHEF, where the Φ_F of the ligand (**33** or **34**) is greatly enhanced while the emission wavelength is intact. The second step coordination to afford the dinuclear complex changes the position of the emission band with the Φ_F remaining high. The strategy taken in our study is similar to the very first example of fluorescent heteroditopic ligands, compound **25**, reviewed in this article (*83*). The fluorescence contrasts in terms of emission wavelength and Φ_F between the three coordination states of **33** and **34** are larger than those of previous examples, owing to our ever-improved understanding of the metal coordination-driven photophysical processes in the arylvinyl–bipy and arylalkynyl–bipy systems and a rationally directed design strategy.

4. Summary and outlook

Over the past few years, research on fluorescent heteroditopic ligands for metal ions has intensified. A rapidly expanding knowledge base on coordination chemistry and photophysical processes of fluorescent heteroditopic ligands gained from the investigations of the earlier examples is fuelling the rational design of chemical systems directed at solving practical problems in areas such as sensing and molecular logic functions. In particular, attention has been converging on the development of sensors and probes targeting substances of medical and environmental importance. On the other hand, many studies, including ours, require more thorough investigations to support or revise the postulated mechanisms of coordination-driven photophysical processes. We have begun to realise the complexity of the processes involved in such systems. The intrinsic molecular interactions between metal ions and ligands, as well as environmental effects such as solvent and counterion on the coordination-driven fluorescence modulation mandate the continued, systematic investigations on the fundamental aspects of fluorescent heteroditopic ligands by many in the supramolecular chemistry community, the outcome of which will eventually feed back to benefit the technological developments.

Acknowledgements

This work was supported by the Florida State University through a start-up fund, a New Investigator Research (NIR) grant from the James and Esther King Biomedical Research Program administered by the Florida Department of Health and National Science Foundation (CHE 0809201). Other Zhu group members are gratefully acknowledged for their support of this project.

References

(1) Lehn, J.-M. *Pure Appl. Chem.* **1978**, *50*, 871–892.
(2) Lehn, J.-M. *Pure Appl. Chem.* **1980**, *52*, 2441–2459.
(3) Fenton, D.E.; Casellato, U.; Vigato, P.A.; Vidali, M. *Inorg. Chim. Acta* **1982**, *62*, 57–66.
(4) Mackay, L.G.; Wylie, R.S.; Sanders, J.K.M. *J. Am. Chem. Soc.* **1994**, *116*, 3141–3142.
(5) Chapman, W.H.; Breslow, R. *J. Am. Chem. Soc.* **1995**, *117*, 5462–5469.
(6) Fahrni, C.J.; Pfaltz, A.; Neuburger, M.; Zehnder, M. *Helv. Chim. Acta* **1998**, *81*, 507–524.
(7) Fahrni, C.J.; Pfaltz, A. *Helv. Chim. Acta* **1998**, *81*, 491–506.
(8) Barrios, A.M.; Lippard, S.J. *J. Am. Chem. Soc.* **1999**, *121*, 11751–11757.
(9) He, C.; Lippard, S.J. *J. Am. Chem. Soc.* **2000**, *122*, 184–185.
(10) Sissi, C.; Rossi, P.; Felluga, F.; Formaggio, F.; Palumbo, M.; Tecilla, P.; Toniolo, C.; Scrimin, P. *J. Am. Chem. Soc.* **2001**, *123*, 3169–3170.
(11) Zhu, L.; dos Santos, O.; Koo, C.W.; Rybstein, M.; Pape, L.; Canary, J.W. *Inorg. Chem.* **2003**, *42*, 7912–7920.
(12) Gianneschi, N.C.; Bertin, P.A.; Nguyen, S.T.; Mirkin, C.A.; Zakharov, L.N.; Rheingold, A.L. *J. Am. Chem. Soc.* **2003**, *125*, 10508–10509.
(13) Coughlin, P.K.; Martin, A.E.; Dewan, J.C.; Watanabe, E.-I.; Bulkowski, J.E.; Lehn, J.-M.; Lippard, S.J. *Inorg. Chem.* **1984**, *23*, 1004–1009.
(14) Jazwinski, J.; Lehn, J.-M.; Lilienbaum, D.; Ziessel, R.; Guilhem, J.; Pascard, C. *J. Chem. Soc., Chem. Commun.* **1987**, 1691–1694.
(15) Fabbrizzi, L.; Licchelli, M.; Rabaioli, G.; Taglietti, A. *Coord. Chem. Rev.* **2000**, *205*, 85–108.
(16) Fabbrizzi, L.; Leone, A.; Taglietti, A. *Angew. Chem. Int. Ed.* **2001**, *40*, 3066–3069.
(17) Hortala, M.A.; Fabbrizzi, L.; Marcotte, N.; Stomeo, F.; Taglietti, A. *J. Am. Chem. Soc.* **2003**, *125*, 20–21.
(18) Boiocchi, M.; Bonizzoni, M.; Fabbrizzi, L.; Piovani, G.; Taglietti, A. *Angew. Chem. Int. Ed.* **2004**, *43*, 3847–3852.
(19) Zhong, Z.; Postnikova, B.J.; Hanes, R.E.; Lynch, V.M.; Anslyn, E.V. *Chem. Eur. J.* **2005**, *11*, 2385–2394.
(20) Rebek, J., Jr.; Trend, J.E.; Wattley, R.V.; Chakravorti, S. *J. Am. Chem. Soc.* **1979**, *101*, 4333–4337.
(21) Rebek, J., Jr.; Wattley, R.V. *J. Am. Chem. Soc.* **1980**, *102*, 4853–4854.

(22) Rebek, J., Jr.; Wattley, R.V.; Costello, T.; Gadwood, R.; Marshall, L. *Angew. Chem. Int. Ed. Engl.* **1981**, *20*, 605–606.
(23) Rebek, J., Jr.; Marshall, L. *J. Am. Chem. Soc.* **1983**, *105*, 6668–6670.
(24) Onan, K.; Rebek, J., Jr.; Costello, T.; Marshall, L. *J. Am. Chem. Soc.* **1983**, *105*, 6759–6760.
(25) Rebek, J., Jr. *Acc. Chem. Res.* **1984**, *17*, 258–264.
(26) Rebek, J., Jr.; Costello, T.; Marshall, L.; Wattley, R.; Gadwood, R.; Onan, K. *J. Am. Chem. Soc.* **1985**, *107*, 7481–7487.
(27) Kobuke, Y.; Sumida, Y.; Hayashi, M.; Ogoshi, H. *Angew. Chem. Int. Ed. Engl.* **1991**, *30*, 1496–1498.
(28) Baldes, R.; Schneider, H.-J. *Angew. Chem. Int. Ed. Engl.* **1995**, *34*, 321–323.
(29) Beer, P.D.; Dent, S.W. *Chem. Commun.* **1998**, 825–826.
(30) Takeuchi, M.; Ikeda, M.; Sugasaki, A.; Shinkai, S. *Acc. Chem. Res.* **2001**, *34*, 865–873.
(31) Nabeshima, T.; Yoshihira, Y.; Saiki, T.; Akine, S.; Horn, E. *J. Am. Chem. Soc.* **2003**, *125*, 28–29.
(32) Takebayashi, S.; Ikeda, M.; Takeuchi, M.; Shinkai, S. *Chem. Commun.* **2004**, 420–421.
(33) Baylies, C.J.; Harding, L.P.; Jeffery, J.C.; Riis-Johannessen, T.; Rice, C.R. *Angew. Chem. Int. Ed.* **2004**, *2004*, 4515–4518.
(34) Baylies, C.J.; Riis-Johannessen, T.; Harding, L.P.; Jeffery, J.C.; Moon, R.; Rice, C.R.; Whitehead, M. *Angew. Chem. Int. Ed.* **2005**, *44*, 6909–6912.
(35) Lehn, J.-M.; Rigault, A.; Siegel, J.; Harrowfield, J.; Chevrier, B.; Moras, D. *Proc. Natl Acad. Sci. USA* **1987**, *84*, 2565–2569.
(36) Kramer, R.; Lehn, J.-M.; Marquis-Rigault, A. *Proc. Natl Acad. Sci. USA* **1993**, *90*, 5394–5398.
(37) Funeriu, D.P.; Lehn, J.-M.; Fromm, K.M.; Fenske, D. *Chem. Eur. J.* **2000**, *6*, 2103–2111.
(38) Petitjean, A.; Kyritsakas, N.; Lehn, J.-M. *Chem. Eur. J.* **2005**, *11*, 6818–6828.
(39) Cheney, J.; Lehn, J.-M.; Sauvage, J.P.; Stubbs, M.E. *J. Chem. Soc., Chem. Commun.* **1972**, 1100–1101.
(40) Wiest, R.; Weiss, R. *J. Chem. Soc., Chem. Commun.* **1973**, 678–679.
(41) Gubelmann, M.; Harriman, A.; Lehn, J.-M.; Sessler, J.L. *J. Chem. Soc., Chem. Commun.* **1988**, 77–79.
(42) Gubelmann, M.; Harriman, A.; Lehn, J.-M.; Sessler, J.L. *J. Phys. Chem.* **1990**, *94*, 308–315.
(43) He, C.; Lippard, S.J. *Inorg. Chem.* **2000**, *39*, 5225–5231.
(44) de Silva, A.P.; Gunaratne, H.Q.N.; Gunnlaugsson, T.; Huxley, A.J.M.; McCoy, C.P.; Rademacher, J.T.; Rice, T.E. *Chem. Rev.* **1997**, *97*, 1515–1566.
(45) Ueno, T.; Urano, Y.; Setsukinai, K.-i.; Takakusa, H.; Kojima, H.; Kikuchi, K.; Ohkubo, K.; Fukuzumi, S.; Nagano, T. *J. Am. Chem. Soc.* **2004**, *126*, 14079–14085.
(46) Huston, M.E.; Haider, K.W.; Czarnik, A.W. *J. Am. Chem. Soc.* **1988**, *110*, 4460–4462.
(47) Akkaya, E.U.; Huston, M.E.; Czarnik, A.W. *J. Am. Chem. Soc.* **1990**, *112*, 3590–3593.
(48) Reichardt, C. *Chem. Rev.* **1994**, *94*, 2319–2358.
(49) Lochbrunner, S.; Schultz, T.; Schmitt, M.; Shaffer, J.P.; Zgierski, M.Z.; Stolow, A. *J. Chem. Phys.* **2001**, *114*, 2519–2522.
(50) Fahrni, C.J.; Henary, M.M.; Van Derveer, D.G. *J. Phys. Chem. A* **2002**, *106*, 7655–7663.
(51) Nagaoka, S.-i.; Kusunoki, J.; Fujibuchi, T.; Hatakenaka, S.; Mukai, K.; Nagashima, U. *J. Photochem. Photobiol. A* **1999**, *122*, 151–159.
(52) Santra, S.; Krishnamoothy, G.; Dogra, S.K. *J. Phys. Chem. A* **2000**, *104*, 476–482.
(53) Prieto, F.R.; Rodriguez, M.C.R.; Gonzalez, M.M.; Fernandez, M.A.R. *J. Phys. Chem.* **1994**, *98*, 8666–8672.
(54) Henary, M.M.; Fahrni, C.J. *J. Phys. Chem. A* **2002**, *106*, 5210–5220.
(55) Ogawa, S.; Tsuchiya, S. *Chem. Lett.* **1996**, 709–710.
(56) Takeno, K.; Furuhama, A.; Ogawa, S.; Tsuchiya, S. *J. Chem. Soc., Perkin Trans. 2* **1999**, 1063–1068.
(57) Kadarkaraisamy, M.; Sykes, A.G. *Inorg. Chem.* **2006**, *45*, 779–786.
(58) McFarland, S.A.; Finney, N.S. *J. Am. Chem. Soc.* **2001**, *123*, 1260–1261.
(59) McFarland, S.A.; Finney, N.S. *J. Am. Chem. Soc.* **2002**, *124*, 1178–1179.
(60) Mello, J.V.; Finney, N.S. *Angew. Chem. Int. Ed.* **2001**, *40*, 1536–1538.
(61) Valeur, B.; Pouget, J.; Bourson, J.; Kaschke, M.; Ernesting, N.P. *J. Phys. Chem.* **1992**, *96*, 6545–6549.
(62) Czarnik, A.W.; Ed. *Fluorescent Chemosensors for Ion and Molecule Recognition*; American Chemical Society: Washington, DC, 1992.
(63) Slavik, J. *Fluorescent Probes in Cellular and Molecular Biology*; CRC Press: Boca Raton, FL, 1994.
(64) Desvergne, J.P.; Czarnik, A.W.; Eds.; *Chemosensors of Ion and Molecule Recognition*; Kluwer Academic Publishers: Dordrecht, 1997.
(65) Valeur, B.; Leray, I. *Coord. Chem. Rev.* **2000**, *205*, 3–40.
(66) Kubo, K.; Sakurai, T. *Heterocycles* **2000**, *52*, 945–976.
(67) Rurack, K.; Resch-Genger, U. *Chem. Soc. Rev.* **2002**, *31*, 116–127.
(68) Valeur, B. *Molecular Fluorescence. Principles and Applications*; Wiley-VCH: New York, NY, 2002.
(69) Fages, F.; Desvergne, J.-P.; Bouas-Laurent, H.; Lehn, J.-M.; Konopelski, J.P.; Marsau, P.; Barrans, Y. *J. Chem. Soc., Chem. Commun.* **1990**, 655–658.
(70) Ji, H.-F.; Brown, G.M.; Dabestani, R. *Chem. Commun.* **1999**, 609–610.
(71) Ji, H.-F.; Dabestani, R.; Brown, G.M.; Hettich, R.L. *J. Chem. Soc., Perkin Trans. 2* **2001**, 585–591.
(72) Leray, I.; Asfari, Z.; Vicens, J.; Valeur, B. *J. Chem. Soc., Perkin Trans. 2* **2002**, 1429–1434.
(73) Malval, J.-P.; Leray, I.; Valeur, B. *New J. Chem.* **2005**, *29*, 1089–1094.
(74) Janssen, P.G.A.; Jonkheijm, P.; Thordarson, P.; Gielen, J.C.; Christianen, P.C.M.; van Dongen, J.L.J.; Meijer, E.W.; Schenning, P.H.J. *J. Mater. Chem.* **2007**, *17*, 2654–2660.
(75) Kim, J.S.; Shon, O.J.; Rim, J.A.; Kim, S.K.; Yoon, J. *J. Org. Chem.* **2002**, *67*, 2348–2351.
(76) Casnati, A.; Pochini, A.; Ungaro, R.; Ugozzoli, F.; Arnaud, F.; Fanni, S.; Schwing, M.-J.; Egberink, R.J.M.; de Jong, F.; Reinhoudt, D.N. *J. Am. Chem. Soc.* **1995**, *117*, 2767–2777.
(77) Rudkevich, D.M.; Mercer-Chalmers, J.D.; Verboom, W.; Ungaro, R.; de Jong, F.; Reinhoudt, D.N. *J. Am. Chem. Soc.* **1995**, *117*, 6124–6125.
(78) Kraemer, R. *Angew. Chem. Int. Ed.* **1998**, *37*, 772–773.
(79) Kim, J.S.; Noh, K.H.; Lee, S.H.; Kim, S.K.; Kim, S.K.; Yoon, J. *J. Org. Chem.* **2003**, *68*, 597–600.
(80) de Silva, A.P.; Sandanayake, K.R.A.S. *Chem. Commun.* **1989**, 1183–1185.
(81) Ji, H.-F.; Dabestani, R.; Brown, G.M.; Sachleben, R.A. *Chem. Commun.* **2000**, 833–834.
(82) Kim, S.K.; Lee, S.H.; Lee, J.Y.; Lee, J.Y.; Bartsch, R.A.; Kim, J.S. *J. Am. Chem. Soc.* **2004**, *126*, 16499–16506.

(83) Rurack, K.; Bricks, J.L.; Schulz, B.; Maus, M.; Reck, G.; Resch-Genger, U. *J. Phys. Chem. A* **2000**, *104*, 6171–6188.
(84) de Silva, A.P.; Gunaratne, H.Q.N. *J. Chem. Soc., Chem. Commun.* **1990**, 186–188.
(85) de Silva, A.P.; Gunaratne, H.Q.N.; Maguire, G.E.M. *J. Chem. Soc., Chem. Commun.* **1994**, 1213–1214.
(86) de Silva, A.P.; Gunaratne, H.Q.N.; Gunnlaugsson, T.; Nieuwenhuyzen, M. *Chem. Commun.* **1996**, 1967–1968.
(87) Rurack, K.; Resch-Genger, U.; Bricks, J.L.; Spieles, M. *Chem. Commun.* **2000**, 2103–2104.
(88) Fahrni, C.J.; Yang, L.; Van Derveer, D.G. *J. Am. Chem. Soc.* **2003**, *125*, 3799–3812.
(89) Grdenic, D.; Kamenar, B.; Zezelj, V. *Acta Cryst.* **1979**, *B35*, 1889–1890.
(90) Tung, J.-Y.; Liau, B.-C.; Elango, S.; Chen, J.-H.; Hsieh, H.-Y.; Liao, F.-L.; Wang, S.-L.; Hwang, L.-P. *Inorg. Chem. Commun.* **2002**, *5*, 150–155.
(91) Fedorov, Y.V.; Fedorova, O.A.; Andryukhina, E.N.; Gromov, S.P.; Alfimov, M.V.; Kuzmina, L.G.; Churakov, A.V.; Howard, J.A.K.; Aaron, J.-J. *New J. Chem.* **2003**, *27*, 280–288.
(92) Rurack, K.; Koval'chuck, A.; Bricks, J.L.; Slominskii, J.L. *J. Am. Chem. Soc.* **2001**, *123*, 6205–6206.
(93) Rettig, W. *Top. Curr. Chem.* **1994**, *169*, 253–299.
(94) Rurack, K.; Rettig, W.; Resch-Genger, U. *Chem. Commun.* **2000**, 407–408.
(95) Ohshima, A.; Momotake, A.; Arai, T. *Tetrahedron Lett.* **2004**, *45*, 9377–9381.
(96) Ohshima, A.; Momotake, A.; Arai, T. *Sci. Tech. Adv. Mat.* **2005**, *6*, 633–643.
(97) Zhang, L.; Dong, S.; Zhu, L. *Chem. Commun.* **2007**, 1891–1893.
(98) Li, Y.Q.; Bricks, J.L.; Resch-Genger, U.; Spieles, M.; Rettig, W. *J. Phys. Chem. A* **2006**, *110*, 10972–10984.
(99) Wilson, J.N.; Bunz, U.H.F. *J. Am. Chem. Soc.* **2005**, *127*, 4124–4125.
(100) Zucchero, A.J.; Wilson, J.N.; Bunz, U.H.F. *J. Am. Chem. Soc.* **2006**, *128*, 11872–11881.
(101) Abe, A.M.M.; Helaja, J.; Koskinen, A.M.P. *Org. Lett.* **2006**, *8*, 4537–4540.
(102) Yuasa, J.; Fukuzumi, S. *J. Am. Chem. Soc.* **2006**, *128*, 15976–15977.
(103) Yuasa, J.; Fukuzumi, S. *J. Am. Chem. Soc.* **2008**, *130*, 566–575.
(104) Licchelli, M.; Linati, L.; Biroli, A.O.; Perani, E.; Poggi, A.; Sacchi, D. *Chem. Eur. J.* **2002**, *8*, 5161–5169.
(105) Zhou, Y.; Xiao, Y.; Qian, X. *Tetrahedron Lett.* **2008**, *49*, 3380–3384.
(106) Huang, J.-H.; Wen, W.-H.; Sun, Y.-Y.; Chou, P.-T.; Fang, J.-M. *J. Org. Chem.* **2005**, *70*, 5827–5832.
(107) Suzuki, T. *Inorg. Chim. Acta* **2006**, *359*, 2431–2438.
(108) Boelrijk, A.E.M.; Neenan, T.; Reekijk, J. *J. Chem. Soc., Dalton Trans.* **1997**, 4561–4570.
(109) Catalano, V.J.; Kar, H.M.; Bennett, B.L. *Inorg. Chem.* **2000**, *39*, 121–127.
(110) He, C.; Lippard, S.J. *Inorg. Chem.* **2001**, *40*, 1414–1420.
(111) Basato, M.; Biffis, A.; Martinati, G.; Tubaro, C.; Graiff, C.; Tiripicchio, A.; Aronica, L.A.; Caporusso, A.M. *J. Organomet. Chem.* **2006**, *691*, 3464–3471.
(112) Tanaka, K.; Miura, T.; Umezawa, N.; Urano, Y.; Kikuchi, K.; Higuchi, T.; Nagano, T. *J. Am. Chem. Soc.* **2001**, *123*, 2530–2536.
(113) Urano, Y.; Kamiya, M.; Kanda, K.; Ueno, T.; Hirose, K.; Nagano, T. *J. Am. Chem. Soc.* **2005**, *127*, 4888–4894.
(114) de Silva, A.P.; Gunaratne, H.Q.N.; Habib-Jiwan, J.-L.; McCoy, C.P.; Rice, T.E.; Soumillion, J.-P. *Angew. Chem. Int. Ed. Engl.* **1995**, *34*, 1728–1731.
(115) Lim, N.C.; Bruckner, C. *Chem. Commun.* **2004**, 1094–1095.
(116) O'Connor, N.A.; Sakata, S.T.; Zhu, H.; Shea, K.J. *Org. Lett.* **2006**, *8*, 1581–1584.
(117) Huang, S.; Clark, R.J.; Zhu, L. *Org. Lett.* **2007**, *9*, 4999–5002.
(118) Zhang, L.; Clark, R.J.; Zhu, L. *Chem. Eur. J.* **2008**, *14*, 2894–2903.
(119) Zhang, L.; Whitfield, W.A.; Zhu, L. *Chem. Commun.* **2008**, 1880–1882.
(120) Zhang, L.; Zhu, L. *J. Org. Chem.* **2008**, *73*, 8321–8330.
(121) de Silva, S.A.; Zavaleta, A.; Baron, D.E.; Allam, O.; Isidor, E.V.; Kashimura, N.; Percapio, J.M. *Tetrahedron Lett.* **1997**, *38*, 2237–2240.
(122) Blackburn, C.; Bai, M.; LeCompte, K.A.; Langmuir, M.E. *Tetrahedron Lett.* **1994**, *35*, 7915–7918.
(123) Henary, M.M.; Wu, Y.; Fahrni, C.J. *Chem. Eur. J.* **2004**, *10*, 3015–3025.